

# Synthesis, Characterization, and Nonlinear Optical Properties of Hybridized CdS–Polystyrene Nanocomposites

H. Du, G. Q. Xu, and W. S. Chin\*

Department of Chemistry, National University of Singapore, 3 Science Drive 3, Singapore 117543

L. Huang and W. Ji

Department of Physics, National University of Singapore, 3 Science Drive 3, Singapore 117543

Received July 23, 2001. Revised Manuscript Received July 11, 2002

Hybrid composites of CdS nanoparticles embedded in sulfonated polystyrene (PS) matrixes have been prepared and characterized. The  $-\text{SO}_3^-$  groups acted as the coordination sites for cadmium ion aggregations and nanosized CdS particles were successfully grown in situ at these sites with the release of  $\text{S}^{2-}$  ions from thioacetamide. The density and size of the nanoparticles were found to be a function of the sulfonate content of PS and the concentration of  $\text{Cd}^{2+}$  feed ions used. Ionic clusterings within the polymer matrix occurred at a sulfonate content of 9.9 mol % and has provided a confined medium for particle growth in uniform size. The optical properties of the prepared CdS–PS hybrid composites were characterized by linear absorption and fluorescence spectra. Z-scan measurement was also employed to investigate the nonlinear optical properties at a wavelength of 532 nm. The results showed that the nonlinear refractive index of the composite varies with the input irradiance, thus indicating not just third-order but possible higher order nonlinearity.

## Introduction

Recently, the synthesis of polymeric matrixes embedded with nanoparticles has attracted much interest in the field of nanomaterials.<sup>1–6</sup> Polymers are considered a good choice as host materials, because they can be designed to yield a variety of bulk physical properties, and they normally exhibit long-term stability and possess flexible reprocessability. This new class of organic–inorganic composites or hybrid materials may afford potential applications in molecular electronics, optics, photoelectrochemical cells, solvent-free coatings, etc.<sup>7</sup> Interesting properties such as fluorescence, electroluminescence, and optical nonlinearity have already been observed.<sup>3,5,6,8,9</sup> Nonlinear optical materials are expected to be important in future high-speed com-

munication networks as all-optical switching, wavelength manipulation, and signal processing devices.<sup>10</sup>

Various approaches have been employed to prepare nanoparticle/polymer composites. The simplest approach involves spin-casting the preprepared nanoparticles together with polymer dissolved in a suitable solvent. This process mixes the two components in solution phase and has been used in the electroluminescence studies of CdSe in poly(*N*-vinylcarbazole) by various groups.<sup>5,6,11</sup> However, the procedure inevitably introduces capping molecules employed in the preprepared nanoparticles into the composites<sup>12</sup> and also requires the selection of a suitable solvent for both the nanoparticles and the chosen polymer matrix.

Another approach uses polymer films containing ionic functionals, which can ion exchange with the precursor salt solution of the nanoparticles.<sup>13–16</sup> When the nanoparticles are eventually formed in situ, a direct encapsulation within the polymer films is thus effected. Wang Y. et al.<sup>13–15</sup> have reported a large third-order nonlin-

\* Corresponding author. Telephone: 65-874-8031. FAX: 65-779-1691. E-mail: chmcws@nus.edu.sg.

- (1) Pyun, J.; Matyjaszewski, K. *Chem. Mater.* **2001**, *13*, 3436.
- (2) Thurn-Albrecht, T.; Schotter, J.; Kastle, G. A.; Emley, N.; Shibauchi, T.; Krusin-Elbaum, L.; Guarini, K.; Black, C. T.; Tuominen, M. T.; Russell, T. P. *Science* **2000**, *290*, 2126.
- (3) Winiarz, J. G.; Zhang, L. M.; Lal, M.; Friend, C. S.; Prasad, P. N. *J. Am. Chem. Soc.* **1999**, *121*, 5287.
- (4) Moffitt, M.; Vali, H.; Eisenberg, A. *Chem. Mater.* **1998**, *10*, 1021.
- (5) Dabbousi, B. O.; Bawendi, M. G.; Onitsuka, O.; Rubner, M. F. *Appl. Phys. Lett.* **1995**, *66*, 1316.
- (6) Huynh, W. U.; Peng, X.; Alivisatos, A. P. *Adv. Mater.* **1999**, *11*, 923.
- (7) Antonietti, M.; Goltner, C.; *Angew. Chem., Int. Ed. Engl.* **1997**, *36*, 910.
- (8) Woggon, U.; Bogdanov, S. V.; Wind, O.; Schlaad, K. H.; Pier, H.; Klingshirn, C.; Chatziagorastou, P.; Fritz, H. P. *Phys. Rev. B* **1993**, *48*, 11979.
- (9) Schwerzel, R. E.; Spahr, K. B.; Kurmer, J. P.; Wood, V. E.; Jenkins, J. A. *J. Phys. Chem. A* **1998**, *102*, 5622.

(10) Cotter, D.; Manning, R. J.; Blow, K. J.; Ellis, A. D.; Kelly, A. E.; Nesset, D.; Phillips, I. D.; Poustie, A. J.; Rogers, D. C. *Science* **1999**, *286*, 1523.

- (11) Wang, Y.; Herron, N. *J. Lumin.* **1996**, *70*, 48.
- (12) Wang, S.; Yang, S.; Yang, C.; Li, Z.; Wang, J.; Ge, W. *J. Phys. Chem. B* **2000**, *104*, 11853.
- (13) Hilinski, E. F.; Lucas, P. A.; Wang, Y. *J. Chem. Phys.* **1988**, *89*, 3435.
- (14) Wang, Y.; Suna, A.; McHugh, J.; Hilinski, E. F.; Lucas, P. A.; Johnson, R. D. *J. Chem. Phys.* **1990**, *92*, 6927.
- (15) Wang, Y.; Mahler, W. *Opt. Commun.* **1987**, *61*, 233.
- (16) Yuan, Y.; Fendler, J. H.; Cabasso, I. *Chem. Mater.* **1992**, *4*, 312.

erity of CdS nanocrystallites embedded in Nafion films using this method. Incorporation of CdS nanoparticles into polymer-blend membranes of poly(styrenephosphonate diethyl ester) (PSP) and cellulose acetate (CA) has also been reported.<sup>16</sup> In this case, the CdS particles may be incorporated into two different regions, i.e., the homogeneous amorphous blend region or the interface region between the CA crystallites and the blend.<sup>16</sup>

Using a guest–host approach, Olshavsky et al.<sup>17</sup> have attempted to exploit the ion-transporting ability of polyphosphazene matrix to control the growth of particles. Nanometer-sized CdS particles have been successfully encapsulated in their polymer composites, although particle size dispersity was not significantly controlled. On the other hand, Shen et al.<sup>18,19</sup> have reported the synthesis of PbS and ZnS nanocomposites via the microgels of Pb– or Zn–methylacrylate, which were then copolymerized into polystyrene matrix. In a recent paper, Pavel et al. reported<sup>20</sup> an elegant one-pot synthesis of nanoparticle/polymer composite via a reverse micelles method using polymerizable surfactant system.

While much effort has been directed to the synthesis of polymer/nanoparticles hybrid materials, a challenge still remains in producing size-tunable nanoparticles that are free from other capping or surfactant molecules, by using appropriate polymers as stabilizers. The stability and the optoelectronic properties of the composites during applications are still subjects for improvement.

In this paper, we report a simple approach to incorporate CdS nanoparticles into a polystyrene (PS) network. We make use of the unique microstructure formed in the network due to clustering of ionic groups<sup>21</sup> such as  $\text{SO}_3^-$  as a confined medium to synthesize the nano-sized particles. We found that the density and the size of the CdS nanoparticles produced can be controlled by varying the degree of sulfonate content of PS and the concentration of feed  $\text{Cd}^{2+}$  ions. The resultant CdS–PS hybrid composites can be redissolved in organic solvent or cast into homogeneous transparent film. We investigated the growth and morphology of the nanoparticles and characterized the linear absorption and fluorescence properties of the composites. The nonlinear optical properties of the composites in different concentrations were also measured through a Z-scan technique at various input irradiances. The third and higher order nonlinear refractive index of the composites were observed, and the origins of the observed nonlinear refraction are discussed.

## Experimental Section

**Sulfonation of Polystyrene.** Polystyrene (PS) was purchased from Aldrich with  $M_w$  of ca. 230 000 and  $M_n$  of ca. 140 000. Sulfonation with acetyl sulfate was carried out following the procedures reported in the literature.<sup>22</sup> Acetyl sulfate was obtained by mixing concentrated sulfuric acid (96%) with acetic anhydride in a molar ratio of 1/1.6 in an ice

bath. The mixture was allowed to react at room temperature for 10 min and then diluted with 1,2-dichloroethane to a concentration of 1.0 M acetyl sulfate. The commercial polymer (10 g) was then dissolved in 1,2-dichloroethane (50 mL) and mixed with a suitable amount of acetyl sulfate solution under stirring. The reaction lasted 5 h at 50 °C, and the resulting sulfonated PS was precipitated with hexane, followed by washing repeatedly with ethanol and drying.

**Preparation of CdS–PS Hybrid Composites.** About 1 g of sulfonated PS was dissolved in 30 mL of mixed solvent of 1,2-dichloroethane and dimethylformide (DMF). A measured amount of cadmium acetate was dissolved in 3 mL of DMF and added into the polymer solution under stirring for 1.5 h. The solution was then heated to 70 °C in a water bath, and thioacetamide (S/Cd molar ratio was kept at 2) in DMF was slowly added in drops. After an hour of reaction, the solution turned yellowish and was cooled to room temperature. The yellow composite was precipitated by hexane, washed with ethanol several times, and dried.

**Characterization.** The sulfonate content of PS was determined in the following ways. To perform titration, 0.2 g of sulfonated PS was dissolved in a mixture of 15 mL of toluene and 2 mL of ethanol. The solution was titrated with a standardized methanol solution of potassium hydroxide, using phenolphthalein as the indicator. Elemental analysis (EA) was also carried out with a Perkin-Elmer CHNS/O 2400 Analyzer Series II instrument. Infrared spectra were recorded with a Bio-Rad FT-IR spectrometer FTS 165.

The morphology and distribution of CdS particles were inspected with a transmission electron microscope (TEM, JEM-100CXII). The hybrid composite was dissolved in DMF, and a drop of the solution was placed on a carbon-coated copper grid that was left to dry before transferring into the TEM sample chamber. Micrographs were taken at an acceleration voltage of 100 kV. UV absorption spectra were recorded on a Shimadzu spectrofluorophotometer RF-5000 using samples in DMF solution. Fluorescence properties of the composite solutions were measured by a Perkin-Elmer LS-50B luminescence spectrometer with excitation at 400 nm. Powder X-ray diffraction (XRD) patterns were recorded by using  $\text{Cu K}\alpha$  irradiation on a Siemens D5005 X-ray diffractometer.

**Z-Sscan Measurements for CdS–PS Hybrid Composite.** A Nd:YAG laser (Spectro Physics DRC-3) was used to produce linearly polarized incident pulses of 7-ns duration (fwhm) at a wavelength of 532 nm. Several neutral density filters were placed in front of the laser to regulate the pulse energy. The laser pulses then passed through a spatial filter formed by two focusing mirrors ( $f = 50$  cm) and a pinhole 200  $\mu\text{m}$  in diameter. The laser beam transmitted through the spatial filter was a nearly Gaussian beam. After hitting a beam splitter, the laser beam was divided into two parts: the reflected part was taken as a reference, while the transmitted part was focused through the sample by a focusing mirror ( $f = 25$  cm). The pulse energies in front of and behind the sample were monitored by two energy detectors (Laser Precision RjP-735 Probes). In the Z-scan measurements with closed aperture, an aperture was placed between the sample and the detector. The aperture was adjusted so that the aperture transmittance was 30%. The outputs recorded by the two detectors were fed into a computer through an IEEE interface. The beam waist of the laser pulse working at a 10-Hz repetition rate was about 40  $\mu\text{m}$ .

All measurements were conducted at room temperature and the composite was dissolved in DMF at different concentrations. Each sample was contained in a 1-cm-thick quartz cuvette and mounted on a translation stage controlled by a computer that moved the sample along the Z-axis. The computer was also programmed to trigger the laser pulses with intervals.

## Results and Discussion

**Sulfonation of PS and Growth of CdS Nanoparticles in PS Matrix.** In the attempt to incorporate Cd

(17) Olshavsky, M. A.; Allcock, H. R. *Chem. Mater.* **1997**, *9*, 1367.

(18) Gao, M.; Yang, Y.; Yang, B.; Bian, F.; Shen, J. *J. Chem. Soc. Chem. Commun.* **1994**, 2779.

(19) Yang, Y.; Huang, J.; Liu, S.; Shen, J. *J. Mater. Chem.* **1997**, *7*, 131.

(20) Pavel, F. M.; Mackay, R. A. *Langmuir* **2000**, *16*, 8568.

(21) Eisenberg, A.; King, M. (Eds.) *Ion-Containing Polymers*; Academic Press: New York, 1977.

(22) Thaler, M. A. *Macromolecules* **1983**, *16*, 623.

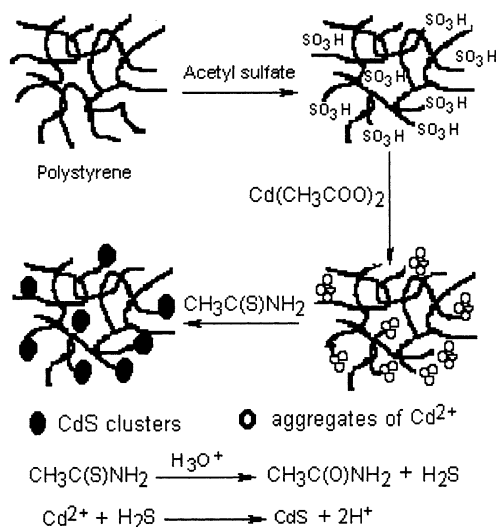
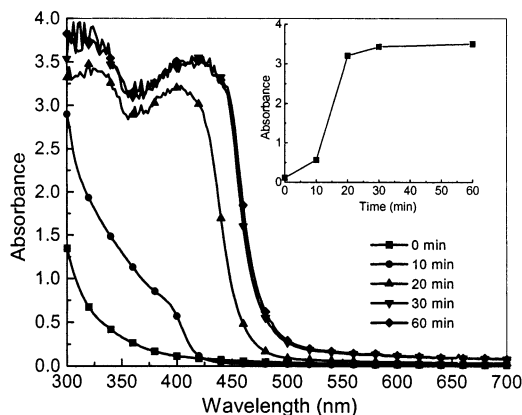
**Table 1. Sulfonate Contents and Weight Percentages of CdS Nanoparticles Embedded in the CdS–PS Hybrid Composites**

sample	sulfonate content SO <sub>3</sub> H/styrene mol %		Cd <sup>2+</sup> /SO <sub>3</sub> H feed ratio		CdS/composite wt % (EA <sup>a</sup> )
	titration	EA <sup>a</sup>	molar ratio	wt %	
A1	3.71	3.66	0.5	2.10	1.77
A2	av = 3.7		1	4.10	4.02
A3			2	7.89	7.94
B1	10.29	9.60	0.5	6.31	3.88
B2	av = 9.9		1	11.87	8.40
B3			2	21.20	16.92

<sup>a</sup> EA: elemental analysis.

ions into the PS network, we first functionalized PS lightly with sulfonic groups. A comparison between IR spectra of the PS samples before and after sulfonation had indicated a weak  $\nu(\text{SO}_2)$  stretching mode<sup>23</sup> at 1126  $\text{cm}^{-1}$  in the later, confirming the successful incorporation of the sulfonic groups. Samples with different extents of sulfonation could be prepared by changing the feed ratio of acetyl sulfate. The sulfonate content, expressed as the molar percentage of SO<sub>3</sub>H/styrene, was determined by titration and elemental analysis (EA), respectively. The two sets of values were in fair agreement with each other. In Table 1, we presented two batches of samples, labeled as A and B for the average fraction of sulfonation at  $\sim 3.7$  and 9.9 mol %, respectively. It has been reported that, for ionic content above some critical value of about 5–6 mol %, ionic groups in PS will form a dispersed phase of clusters due to aggregation, while at lower ionic contents, ion pairs or multiplets may be prevalent and act as cross-linking sites that restrict molecular motion.<sup>21</sup> Our sample batch B thus represented an example of the former and sample batch A an example of the later case.

The nucleation of Cd<sup>2+</sup> ions within the sulfonated PS matrix was carried out in solution through ion exchange with the H<sup>+</sup> ions of the sulfonic groups. Cd<sup>2+</sup> ions aggregated at the sites of sulfonic clusters distributed within the polymer network. The formation of CdS took place in situ when S<sup>2-</sup> ions were released by thioacetamide (TAA) upon heating. The decomposition mechanism of TAA has been described before,<sup>24</sup> and the overall reaction of our preparation is schematically shown in Figure 1. It is noted that the decomposition of TAA is readily induced in our procedure, probably due to the slight acidic medium after Cd<sup>2+</sup> ion exchange with H<sup>+</sup> of the sulfonate groups. The rate of generation of S<sup>2-</sup> from TAA is known to depend on temperature,<sup>24</sup> but higher temperatures may mobilize the ionic clusters in our polymer and cause agglomeration to form large particles. By monitoring the UV absorption spectra during the process of CdS formation, we have found that a reasonable growth rate could be achieved at 70 °C. An onset in the UV spectra was noticeable after just about 10 min of introduction of TAA (Figure 2), and the growth was nearly completed after  $\sim 30$  min. As expected, the absorption peak red-shifted as the particles grow larger with time. A plot of UV absorbance at 400 nm versus time (inset of Figure 2) seemed to suggest a

**Figure 1.** Schematic preparation of CdS nanoparticles within the sulfonated PS matrix.**Figure 2.** UV spectra monitoring the growth of CdS particles within the PS matrix as a function of reaction time. The inset shows the absorbance at 400 nm versus time.

slight induction period prior to a rapid growth of the nanoparticles. The brief induction period may be indicative of the diffusion of S<sup>2-</sup> ions through the complex polymer network before reaching the Cd<sup>2+</sup> cluster sites to form a steady-state supply of S<sup>2-</sup> ions. In our preparation, excess S<sup>2-</sup> ions (two times the molar amount of Cd<sup>2+</sup>) were used to ensure complete conversion to CdS.

To investigate the effect of changing Cd<sup>2+</sup> feed ratios, we divided the sulfonated PS sample batches A and B into three portions, respectively, and prepared three series of samples with the Cd<sup>2+</sup>/SO<sub>3</sub>H ratio increasing from 0.5 to 1 to 2. The actual weight percentages of CdS nanoparticles finally incorporated into the composites were determined by EA and are shown in Table 1. Thus, composites containing 2–17 wt % of CdS nanoparticles could be conveniently prepared by varying the sulfonate content of the polymer as well as the Cd<sup>2+</sup>/SO<sub>3</sub>H feed ratio. These determined values were expected to be slightly lower than the feed ratios, since loss of some CdS particles during preparation is inevitable. It is interesting to note, however, that while the loss was 0.05–0.33% for samples with average sulfonate content of 3.7 mol % (i.e., A1–A3), it was consistently higher (i.e., 3–4%) for samples with sulfonate content of 9.9 mol % (B1–B3). We suspect this is due to the different

(23) Zhu, X.; Elomaa, M.; Sundholm, F.; Lochmuller, C. H. *Polym. Degradation Stability* **1998**, *62*, 487.

(24) Celikkaya, A.; Akinc, M. *J. Am. Ceram. Soc.* **1990**, *73*, 245.



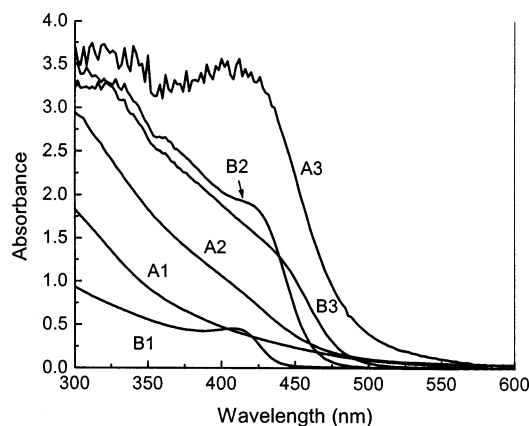


**Figure 3.** UV absorption spectra of CdS–PS hybrid composites synthesized with different feed ratios of Cd<sup>2+</sup> (see Table 1). The average fraction of sulfonation is 3.7 and 9.9 mol % for batches A and B, respectively.

microstructures present in the polymer network, since samples with ionic content lower than 5–6 mol % may be more cross-linked due to ion pairs or multiplets formation.<sup>21</sup> The nanoparticles formed may thus be relatively more entangled within the network of samples A1–A3.

The as-synthesized hybrid CdS–PS composites could be cast into optically transparent thin films, but those with higher CdS wt % showed a tint of yellow color. These films were homogeneous and showed no phase separation. Differential scanning calorimetry (DSC) measurement found that the glass transition temperature of the sulfonated PS ( $T_g = 116.83$  and  $137.42$  °C for batch A and B, respectively) did not change after doping with the CdS nanoparticles, indicating that the physical properties of the polymer were largely retained. Thermal gravimetric analysis indicated that these composites do not decompose until  $>450$  °C in a N<sub>2</sub> environment. In addition, the optical properties of the embedded CdS nanoparticles are stable and did not show any sign of deterioration after storage under the ambient conditions for more than 6 months. The composites were also found to be photochemically stable after a prolonged period of laser irradiation (vide infra).

**Morphology and Particle Sizes.** The UV absorption spectra of all six samples in DMF are presented in Figure 3. Pure sulfonated PS sample was found to absorb below 300 nm; hence, the absorption between 300 and 600 nm can be attributed to the CdS nanoparticles embedded. It is known that the UV/vis onset absorption of semiconductor nanoparticles is attributed to the band gap absorption, and this will be blue-shifted relative to the bulk due to quantum size confinement effect.<sup>25,26</sup> Thus, Figure 3 shows that the UV thresholds of all samples (except that of A3) are blue-shifted relative to bulk CdS at 512 nm, suggesting the formation of nanometer-sized CdS particles in our samples. It is also noted that, within the same batch of samples A or B, the absorption threshold becomes more blue-shifted as the Cd<sup>2+</sup> feed ratio is decreased. This suggests that the nanoparticle size can be adjusted by changing the feed

ratio of the Cd<sup>2+</sup> ions, as particles of smaller size were formed when a lesser amount of precursor Cd<sup>2+</sup> ions was used in the feed.

Comparing across samples of batches A and B reveals, however, that the UV thresholds of composites B are always lower than those in the corresponding sample of composites A. This is despite the fact that the effective weight percentages of CdS in composites B are always higher. Thus, the UV thresholds of samples B1, B2, and B3 are found at 442, 463, and 492 nm, corresponding to band gaps of 2.80, 2.68, and 2.52 eV, respectively. The average particle size, calculated from the Brus equation based on the effective mass approximation,<sup>25</sup> are 2.3, 2.7, and 5.6 nm, respectively. When compared to the experimental curve of absorption threshold versus particle diameter by Henglein et al.,<sup>26</sup> the average particle sizes of our samples are estimated to be within 3–6 nm.

The morphology and distribution of CdS nanoparticles in the hybrid composites were also investigated using TEM. Some typical TEM images of composites B are presented in Figure 4. It is found that at lower Cd<sup>2+</sup> concentration (sample B1 in Figure 4a), some CdS nanoparticles are loosely distributed within the polymers but some aggregated clusters of varying size can also be found. When the CdS content is increased in sample B2, a higher density of particles is clearly seen in Figure 4b and tiny clusters in spherical shapes are connected together in some areas rich in CdS. Increasing the Cd/SO<sub>3</sub>H ratio to 2 in sample B3 produced a network consisting of CdS clusters uniformly distributed within the entire polymer matrix, as shown in Figure 4c. In the higher magnification image in Figure 4d, CdS particles are found to be connected but with a narrow size distribution. The average sizes of CdS nanoparticles estimated from TEM seemed to agree well with those estimated from the UV absorption threshold, although the clustering of nanoparticles has forbidden more precise distribution to be obtained from TEM analysis.

The limiting mechanism for particle growth in our system is probably the inhibition of diffusion, since the bending or coiled structures of the polymer chains will hinder the diffusion-driven processes within the network. It is also possible that polymer chains may be bridged by connecting to the same nanoparticle, and a multiplicity of such bridged chains and particles could lead to particle clusterings.<sup>27</sup> It is worth noting that relatively smaller and more uniform nanoparticles were formed in composites B, which have a higher sulfonate content compare to composites A. This seems to confirm that the higher ionic content in PS has effected a more efficient clustering of the ionic groups into domains of small size. These randomly distributed ionic domains allow the aggregations of Cd<sup>2+</sup> ions to occur and later effected the growth of CdS nanoparticles within them. At lower ionic contents such as those in composites A, the polymer chains may form more cross-links than domains due to ion pairs or multiplets formation.<sup>21</sup> The restricted molecular motion may still induce nanoparticles formation, but the resultant distribution is found to be not as uniform.

(25) (a) Brus, L. E. *J. Chem. Phys.* **1983**, *79*, 5566. (b) Brus, L. E. *J. Chem. Phys.* **1984**, *80*, 4403.

(26) (a) Henglein, A. *Chem. Rev.* **1989**, *89*, 1861. (b) Spanhel, L.; Haase, M.; Weller, H.; Henglein, A. *J. Am. Chem. Soc.* **1987**, *109*, 5649.

(27) Premachandran, R.; Banerjee, S.; John, V. T.; McPherson, G. L.; Akkara, J. A.; Kaplan, D. L. *Chem. Mater.* **1997**, *9*, 1342.

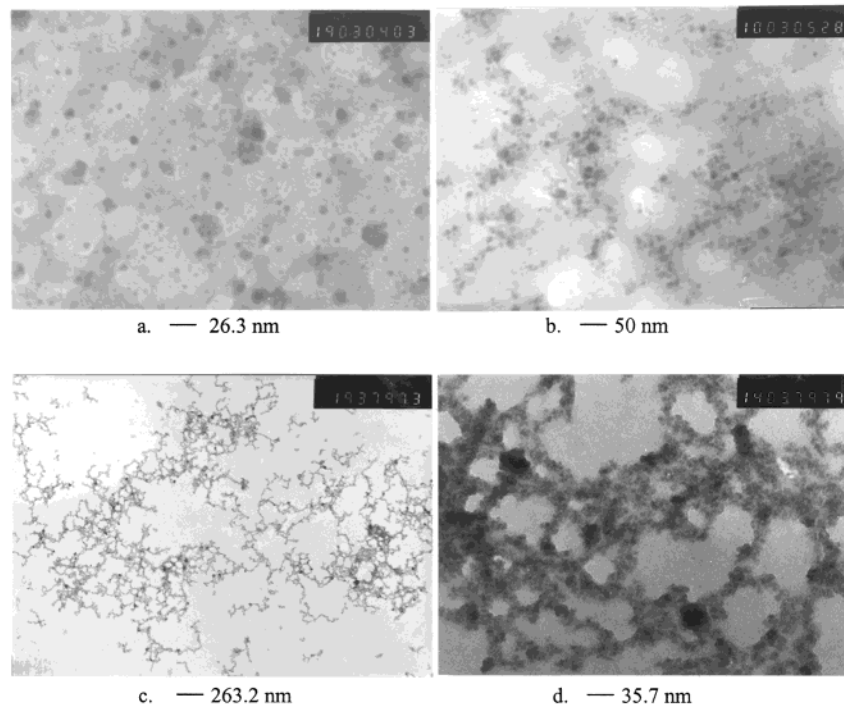


**Figure 4.** TEM images of CdS–PS hybrid composites: (a) B1, (b) B2, (c) B3, and (d) high magnification image of image c.

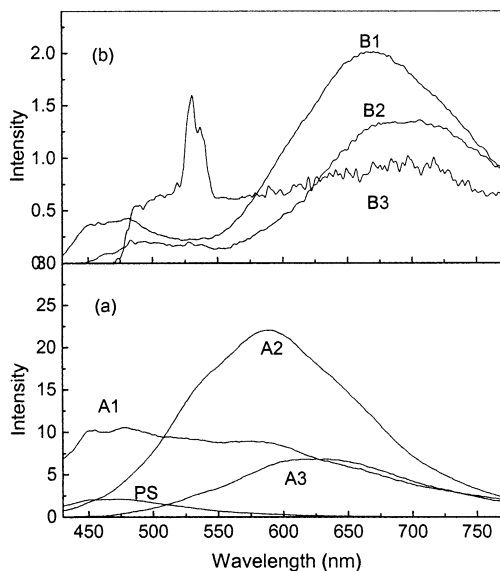


**Figure 5.** Fluorescence spectra of CdS–PS hybrid composites with excitation wavelength at 400 nm: (a) composites A1–A3 and (b) composites B1–B3, all in DMF.

**Fluorescence Property of CdS–PS Hybrid Composites.** The fluorescence spectra of the CdS–PS composites were recorded at an excitation wavelength of 400 nm and presented in Figure 5. In the case of composites B (Figure 5b), two maxima were commonly detected—one broad band that peaks at 650–750 nm and a higher energy emission near the band edge of CdS nanoparticles—although the relative intensities of the two bands vary among the samples. On the other hand, only one broad band at ~550–650 nm is detected for samples A2 and A3 (Figure 5a), while two bands are just discernible in the spectrum of sample A1.

The emission maximum closer to the absorption onset observed in samples A1 and B1–B3 can be assigned to the excitonic fluorescence.<sup>28,29</sup> This band is seen to shift

to higher energy with decreasing concentration of CdS from composites B3–B1. Pure sulfonated PS was found to show very weak fluorescence at ~450–480 nm (labeled as PS in Figure 5a) and thus could not have affected the shift observed here. This blue shift in the emission maximum for smaller CdS nanoparticles is parallel to the shift observed in the UV absorption threshold and is attributable to the size quantization effect.<sup>28</sup> These band-edge emissions are slightly red-shifted from the corresponding absorption thresholds, probably due to the presence of some shallow surface traps.<sup>29,15</sup> The bound excitons in the defect states will exhibit a strong interaction with the free excitons and cause absorption bleaching, which in turn produces the nonlinear optical properties of small CdS particle systems.<sup>12–15</sup>

The broad red emission band that occurs at ~680 nm in samples B1–B3 is commonly observed in CdS nanoparticles and bulk crystals.<sup>13,14,28–31</sup> The most common defects present in these materials are sulfur  $S^{2-}$  vacancies ( $V_S$ ), which are located at 0.63 eV below the conduction band in bulk CdS<sup>13</sup> and can exothermically extract an electron from the valence band. The red emission band is thus attributed to the recombination of an electron trapped in a sulfur vacancy ( $V_S^-$ ) with a hole ( $h_{VB}^+$ ) photogenerated in the valence band.<sup>13,28–30</sup> Among the three samples B1–B3, it is found that the red emission band is relatively enhanced with the decrease of particle size from B3 to B1. This seems to suggest that the larger specific surface area in smaller particles will result in more surface defects that can

(28) Gopidas, K. R.; Kamat, P. V. *Proc. Indian Acad. Sci.* **1993**, *105*, 505

(29) Misawa, K.; Yao H.; Hayashi, T.; Kobayashi, T. *Chem. Phys. Lett.* **1991**, *183*, 113.

(30) Boyle, D. S.; O'Brien, P.; Otway, D. J.; Robbe, O. *J. Mater. Chem.* **1999**, *9*, 725.

(31) Zhao, X. S.; Schroeder, J.; Persans, P. D.; Bilodeau, T. G. *Phys. Rev. B* **1991**, *43*, 12580.

easily trap excited electrons or holes.<sup>29,31</sup> Decreased surface area and saturation of sulfur vacancies in sample B3 has largely reduced this red-shifted recombination. It is worth pointing out that the band-edge emission peak is also relatively sharper and more distinct in sample B3, with a fwhm of just  $\sim 35$  nm. A similarly distinct peak has also been reported by Misawa et al. for their samples prepared with the gas-diffusion method, and this may be attributed to the relatively uniform size of the nanoparticles synthesized.<sup>29</sup>

It is interesting to note that an orange-green emission at  $\sim 550$ – $650$  nm is detected instead for samples A1–A3 (Figure 5a). This observation seems to indicate a slightly different growth condition in composites A and B, again suggesting a different microstructure network in these two batches. A similar emission has also been observed for CdS particles embedded in polymer-blend membranes<sup>16</sup> and glass composites.<sup>31</sup> The exact origin of this emission is not known, but Zhao et al.<sup>31</sup> have suggested that the main defects in their CdS–glass composites are cadmium vacancies ( $V_{\text{Cd}}$ ), which were estimated to have a binding energy of  $\sim 0.48$  eV. We would like to postulate that such cadmium vacancies could also be induced in our samples, since an excess amount of  $\text{S}^{2-}$  has been used throughout our preparation. On the other hand, sulfur instead of cadmium vacancies are found in composites B, probably because the  $\text{Cd}^{2+}$  ions were well within the ionic clusters protected by the polymer chains. The infiltration of  $\text{S}^{2-}$  ions into the ionic domains did not occur efficiently under the preparation temperature and conditions.

Thus, we have demonstrated above that the ionic clusters in sulfonated polymer matrixes can be used as a very convenient medium to prepare monodispersed nanoparticles. The density and size of the nanoparticles can be easily optimized by adjusting the ionic content and the concentration of feed ions. We believe the approach is general and could be adapted to other polymer and semiconductor types. The hybrid semiconductor–polymer composites as prepared above are stable and free from other capping molecules.<sup>12</sup> They can be redissolved, cast into homogeneous films, or reprocessed for further applications.

In our study, monodispersed and uniform CdS nanoparticles were obtained in sample B3. The optical spectrum of this sample exhibits a particularly sharp band-edge emission (Figure 5b). The magnitude and dispersion of the nonlinear refractive index ( $n_2$ ) of this sample will be of interest because of their importance in applications such as fast optical switching, self-focusing and damage in optical materials, and optical limiting in semiconductors.<sup>32</sup> We have thus used the closed-aperture Z-scan technique to determine the sign and magnitude of  $n_2$  for composite B3 in DMF solution at different input irradiances.

**Nonlinear Optical Properties of CdS–PS Hybrid Composites.** Typical Z-scan curves are shown in Figure 6, demonstrating the characteristic shape for a negative nonlinearity. Assuming that the nonlinear refraction in this sample is only due to the third-order mechanism, we fitted the experiment data (solid line) with the standard Z-scan theory to extract the nonlinear refractive index. Figure 7 showed the relationship between

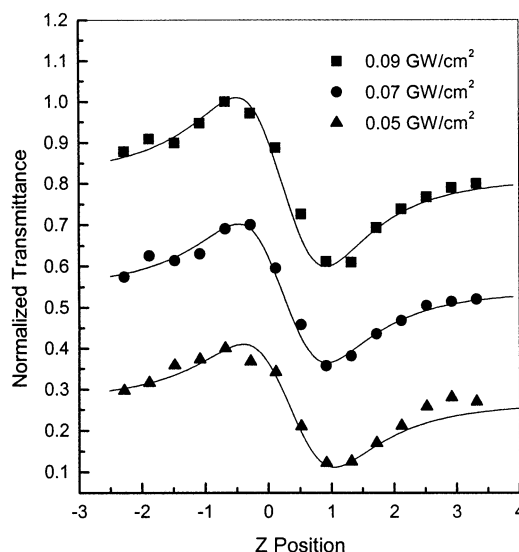


**Figure 6.** Z-scan measurements (close aperture) of the CdS–PS composite at three input irradiances. The laser wavelength is 532 nm and the pulse duration is 7 ns.

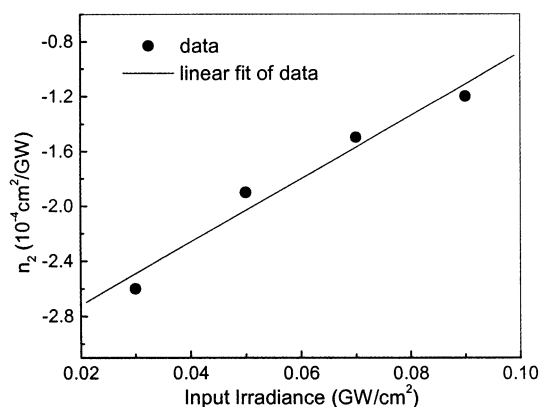


**Figure 7.** The effective nonlinear refractive index of the CdS–PS composite as a function of the input irradiance.

the input irradiance and these index values. From the results of the fitting, we found that the observed nonlinear refractive index increased linearly as the input irradiance decreased and ranged from  $-1.0 \times 10^{-4}$  to  $-3.0 \times 10^{-4}$   $\text{cm}^2/\text{GW}$ . These values are of the same magnitude as Schwerzel's results.<sup>9</sup> They obtained the nonlinear refractive index of capped CdS nanocrystals in an ordered polydiacetylene host at wavelength of 532 nm to be  $1.1 \times 10^{-4}$   $\text{cm}^2/\text{GW}$  using 0.09  $\text{GW}/\text{cm}^2$  laser pulses of 5 ns. In their case, the polydiacetylene host itself has a nonlinear refractive index of about  $-3 \times 10^{-5}$   $\text{cm}^2/\text{GW}$ . In our sample, we could contribute the nonlinearity to the CdS nanoparticles, since the pure sulfonated PS in DMF did not show nonlinear properties. In addition, Wang et al.<sup>14</sup> had performed the pump–probe experiments with ammonia-passivated CdS clusters in polymer. They measured the absorption of CdS at different wavelengths with excitation by a 30 ps laser pulse at 355 nm and obtained the associated changes in refractive index at different wavelengths through the Kramers–Kronig relationship. According to their calculation, the nonlinear refractive index of CdS at 532 nm is  $1.41 \times 10^{-4}$   $\text{cm}^2/\text{GW}$ , which is also in the same range as our results.

Sheik-Bahae et al.<sup>32</sup> and Krauss et al.<sup>34</sup> have presented a scaling rule between the nonlinear refraction



index  $n_2$  and the ratio of the photon energy to the band gap energy ( $h\nu/E_g$ ). Under different  $E_g$  or laser frequency ( $h\nu$ ),  $n_2$  was found to have different values and signs (positive or negative). For bulk CdS, Li et al.<sup>33</sup> had obtained the nonlinear refractive index of  $-(5.3 \pm 0.8) \times 10^{-4} \text{ cm}^2/\text{GW}$  at 532 nm. In our sample, the band gap had been broadened to  $\sim 2.52 \text{ eV}$  and this results in a smaller ratio of  $h\nu/E_g$  and will make the absolute value of nonlinear refractive index smaller. In addition, the nonlinear refraction of CdS nanoparticles may also be affected by the presence of traps and midgap states, as indicated by the emission spectrum in Figure 5b. The free charge and/or the static Stark effect of the electron trapped in these localized states below the band gap can produce a refractive index change. However, since the volume fraction of CdS nanoparticles in our sample is just 2.7%, the nonlinear refraction measured is  $\sim 400$  times of that of the whole sample, say, ranging from  $-4 \times 10^{-2}$  to  $-1.2 \times 10^{-1} \text{ cm}^2/\text{GW}$ . This magnitude is much larger than that of the CdS bulk materials after considering the volume fraction.

At the input irradiance of  $0.05 \text{ GW}/\text{cm}^2$ , we performed the Z-scan measurements at different CdS nanoparticle concentrations at 532 nm, ranging from 0.104 to 0.015 mol/L. Assuming the mechanism of the nonlinear optical properties is only the third-order effect, we fitted the  $n_2$  value at each concentration. The linear relationship between  $n_2$  and the concentration is shown in Figure 8. We can see that the absolute value of  $n_2$  increases linearly, as the particle concentration is higher. The unfixed values of nonlinear refractive index mean that the origin of the nonlinear refraction should not only contribute to the third-order nonlinearity but also to higher orders, which can be caused by the free carrier effect. Also in Figure 7, we can see a linear relationship between the nonlinear refractive index and the input irradiance. This is another proof for the existence of the fifth-order nonlinear optical properties. We may thus give the equation below:

$$n = n_0 + n_{\text{ex}}I = n_0 + (n_2 + n_4)I$$

where  $n$  is the total refractive index,  $n_0$  is the linear refractive index,  $n_{\text{ex}}$  is the effective nonlinear refractive index,  $I$  represents the input laser irradiance,  $n_2$  is the third-order refractive index ( $-2.87 \times 10^{-4} \text{ cm}^2/\text{GW}$ ) and

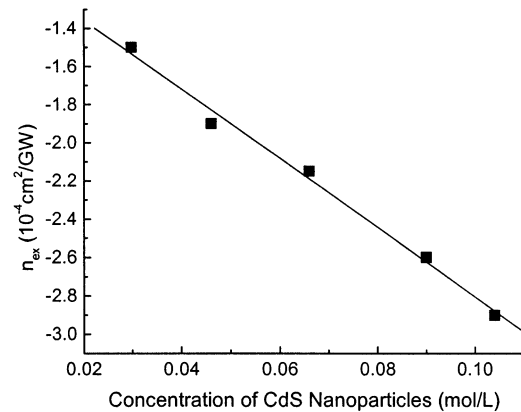


**Figure 8.** The linear relationship between the effective nonlinear refractive index and the concentration of CdS nanoparticles in the solutions.

$n_4$  denotes the fifth-order nonlinearity. Li et al.<sup>33</sup> had found that the free carrier effect (fifth-order nonlinear effect) in bulk CdS is significant for laser pulses of a nanosecond or longer. The lifetime of the carrier had been determined to be 3.6 ns and 0.1 ns, respectively by Li<sup>33</sup> and Lami et al.<sup>35</sup> Further investigations on the free carrier effect in our CdS nanoparticles within the polymer network are now in progress.

### Conclusions

Nanometer-sized semiconductor CdS particles, 2–17 wt %, have been successfully grown within polystyrene matrix that has been lightly substituted with sulfonic group. We have shown that the morphology, the surface properties, and hence the fluorescence properties of the nanoparticles formed are strongly dependent on the sulfonate content of the starting polymer, as well as the  $\text{Cd}^{2+}$  feed ratio. The resulting hybrid composites are highly processable and can be fabricated into films, used as coatings, or even in further polymer blending. The optical nonlinearity measurement via the Z-scan technique showed that the hybrid materials have a effective nonlinear refractive index  $n_2$  ranging from  $-1.0 \times 10^{-4}$  to  $-3.0 \times 10^{-4} \text{ cm}^2/\text{GW}$ , and they vary with the input laser energy as well as the concentration of CdS nanoparticles. It is suggested that not only the third-order nonlinearity but also higher order nonlinear optical properties existed in the CdS–PS composite due to the free carrier effect.

CM010622Z

(32) Sheik-Bahae, M.; Hutchings, D. C.; Hagan, D. J.; Stryland, E. W. V. *IEEE J. Quantum Electron.* **1991**, *27*, 1296.

(33) Li, H. P.; Kam, C. H.; Lam, Y. L.; Ji, W. *Opt. Commun.* **2001**, *190*, 351.

(34) Krauss, T. D.; Wise, F. W. *Appl. Phys. Lett.* **1994**, *65*, 1739.

(35) Lami, J. F.; Hirlimann, C. *Phys. Rev. B* **1999**, *60*, 4763.